Non-invasive intravital imaging of cellular differentiation with a bright red-excitable fluorescent protein

Jun Chu, Russell D Haynes, Stéphane Y Corbel, Pengpeng Li, Emilio González-González, John S Burg, Niloufar J Ataie, Amy J Lam, Paula J Cranfill, Michelle A Baird, Michael W Davidson, Ho-Leung Ng, K Christopher Garcia, Christopher H Contag, Kang Shen, Helen M Blau & Michael Z Lin

SUPPLEMENTARY INFORMATION

Supplementary Figure 1. Amino acid sequences of mNeptune-related FPs

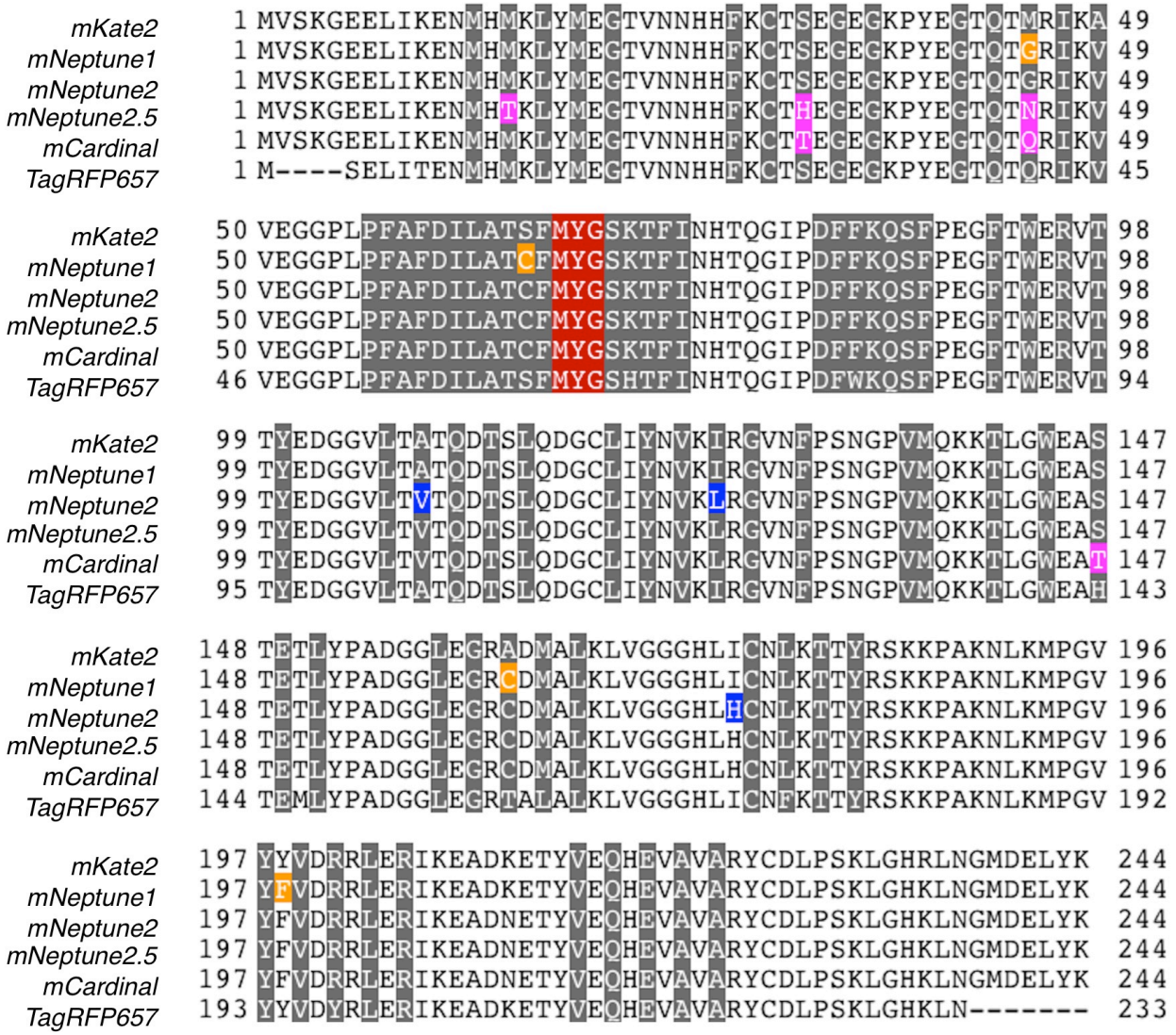

Internal residues are highlighted in gray. Chromophore-forming residues are highlighted in red. Key differences between mKate2 and mNeptune1 are highlighted in orange. Differences between mNeptune1 and mNeptune2 are highlighted in blue. Key differences between mNeptune2 and mNeptune2.5 or mCardinal are highlighted in magenta.

Supplementary Figure 2. Brightness of mNeptune-related proteins *in vitro*

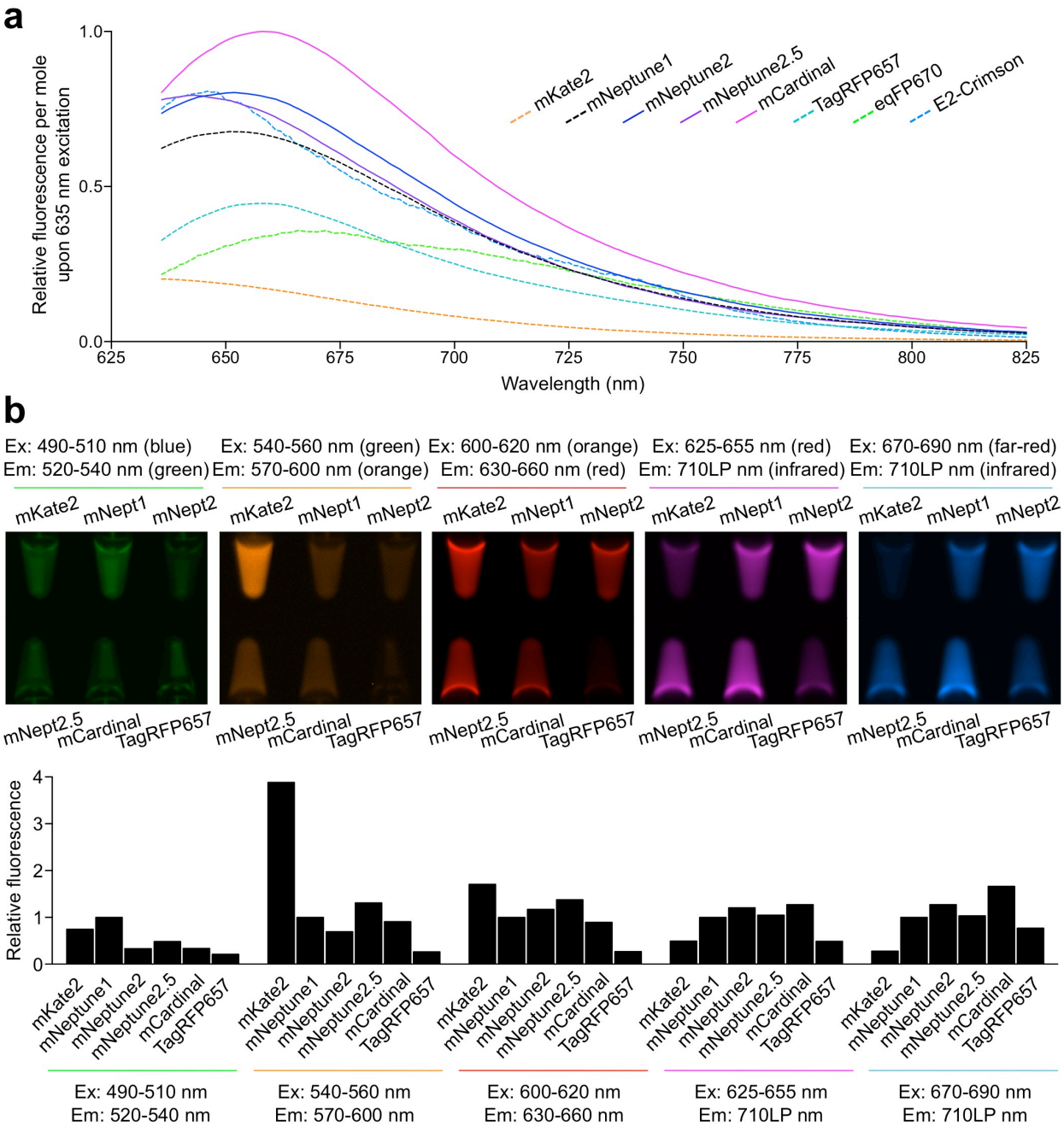

(a) Predicted emission curves upon excitation of equal concentrations of far-red FPs at 635 nm. To accurately reflect the number of photons emitted at each wavelength upon excitation at 635 nm, for each FP, the area under the emission spectrum beyond 635 nm was normalized to the product of extinction coefficient at 635 nm and the quantum yield beyond 635 nm. **(b)** Fluorescence of purified far-red FPs at 1 mg/mL concentration in 200-µL reaction tubes. **(c)** Fluorescence in each image in **(b)** was normalized to mNeptune1 and charted.

Supplementary Figure 3. Two-photon excitation spectra of mCardinal and mNeptune1

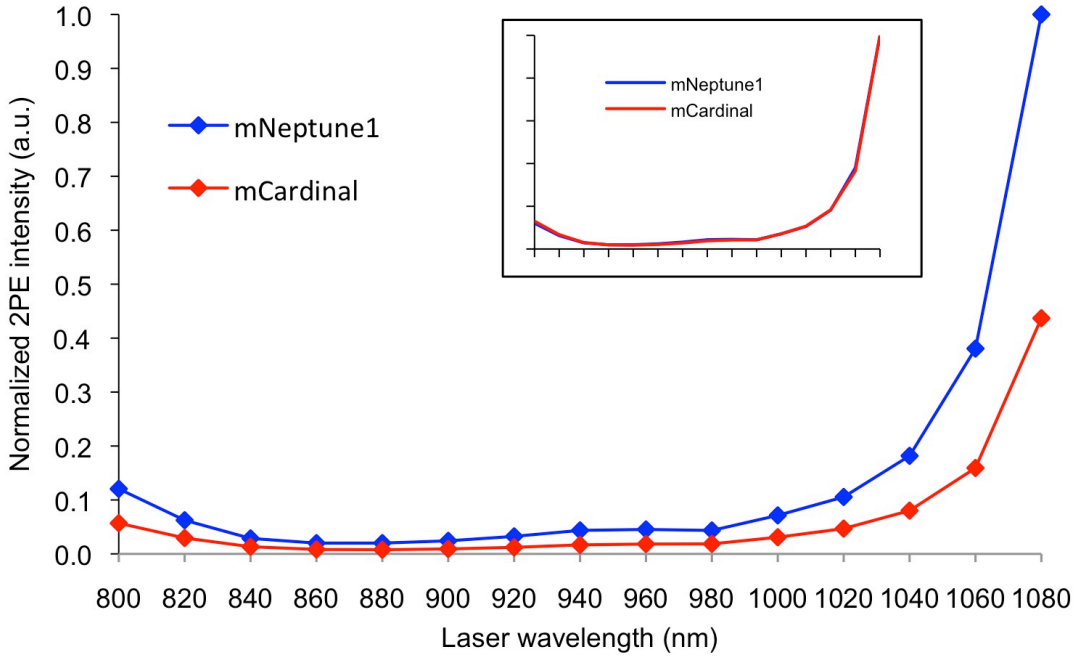

Two-photon excitation spectra were measured on purified proteins with a customized upright microscope (Prairie Technologies) equipped with a Olympus 40× water-immersion objective (NA 0.8), a red-sensitive Hamamatsu PMT and a mode-locked Ti:Sapphire laser (140-fs pulse width; 80 MHz repetition rate; Chameleon Ultra II, Coherent). Briefly, purified proteins in PBS (64 μM or 2 mg/mL) proteins or PBS were loaded into 12-well plate as 1.6 mL/well. The excitation wavelengths from 800 to 1080 nm with 20 nm intervals were changed manually and the power after objective for each wavelength was measured using a power meter. Fluorescence images were acquired through a far-red emission filter HQ 645/70 nm (Chroma) and analyzed in Fiji software. The fluorescence subtracted by PBS was normalized to the square of the power after objective. All fluorescence was normalized to the fluorescence intensity of mNeptune1 at 1080 nm. Inset: fluorescence normalized to respective fluorescence intensity at 1080 nm.

Supplementary Figure 4. Characterization of far-red FPs

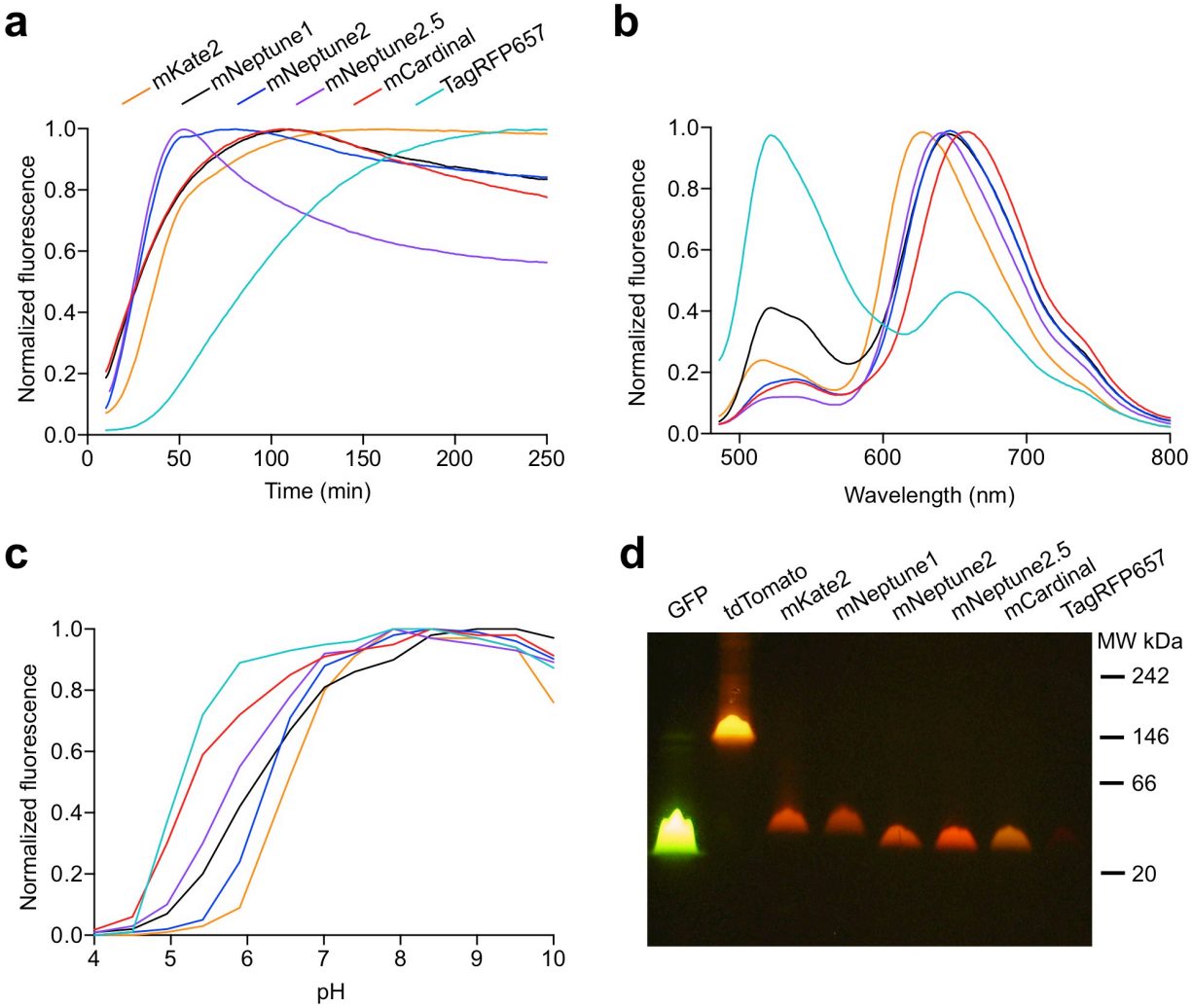

(a) Maturation kinetics at 37°C. Lysates from bacteria expressing FPs in anaerobic conditions were prepared beginning at time 0 and fluorescence measured over time. Mean of triplicate measurements are shown. **(b)** Green and red emissions detected upon excitation with 460 nm light. Colors are as in **(a)**. **(c)** pH dependence of fluorescence. Colors are as in **(a)**. **(d)** Semi-Native PAGE. 10 mg of each protein was electrophoresed on a 4-12% Bis-Tris gel with buffer containing 0.1% SDS, then imaged on a blue LED transilluminator with an orange acrylic filter. GFP and tdTomato were used as the monomeric and dimeric native protein standards, respectively.

Supplementary Figure 5. Photostability of far-red FPs

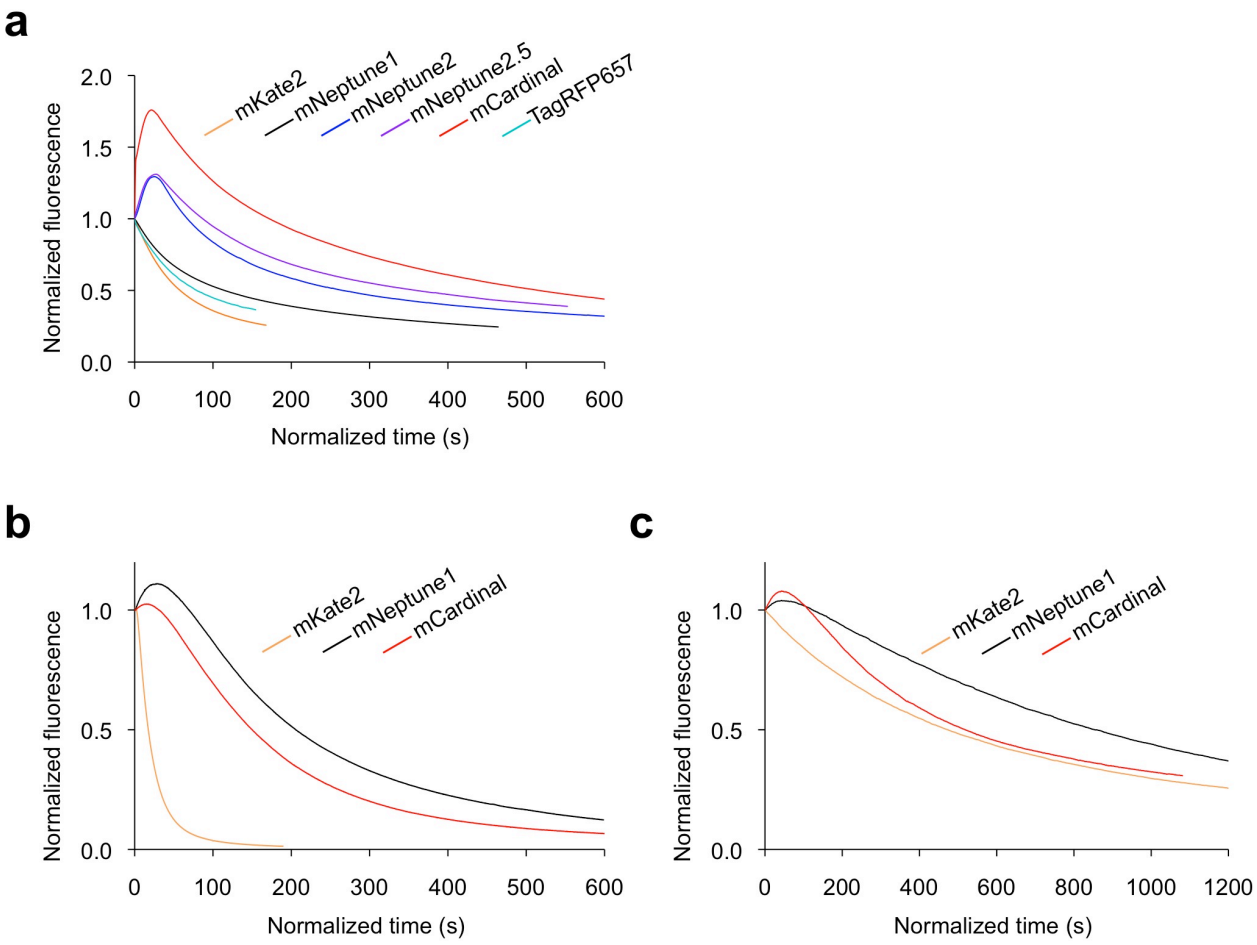

(a) Photobleaching kinetics of purified proteins in oil under arc lamp illumination with a 615/20 nm excitation filter. Each curve is the mean of three independent experiments. **(b, c)** Photobleaching kinetics under arc lamp **(b)** or laser **(c)** illumination of mCardinal, mKate2, and mNeptune1 fused to histone H2B in living HeLa S3 cells. Each curve is the mean of at least three independent experiments.

Supplementary Figure 6. Comparison of mNeptune-related FPs in HeLa cells

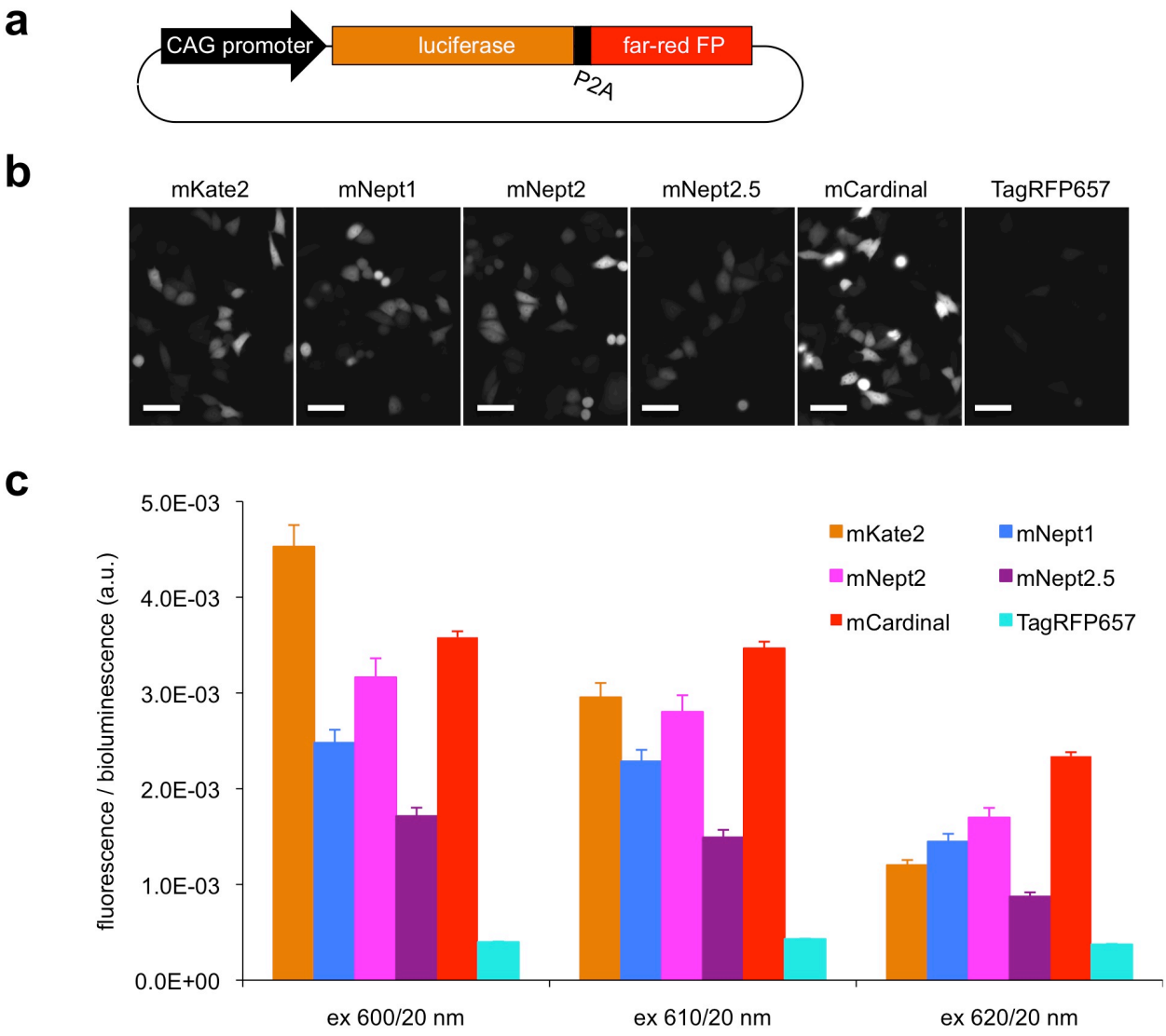

(a) Schematics of the plasmids used for co-expression of far-red FPs and firefly luciferase separated by a P2A peptide. **(b)** Fluorescence images of HeLa cells expressing fluorescent proteins and luciferase. The images were acquired 30 h after transfection with a 615/30 nm excitation filter and a 665/40 nm emission filter. Scale bars, 30 μm. **(c)** Graph of fluorescence intensities normalized to luciferase activity. The data are presented as the mean ± SEM, n = 3.

Supplementary Figure 7. Imaging of far-red FPs in neurons and myocytes

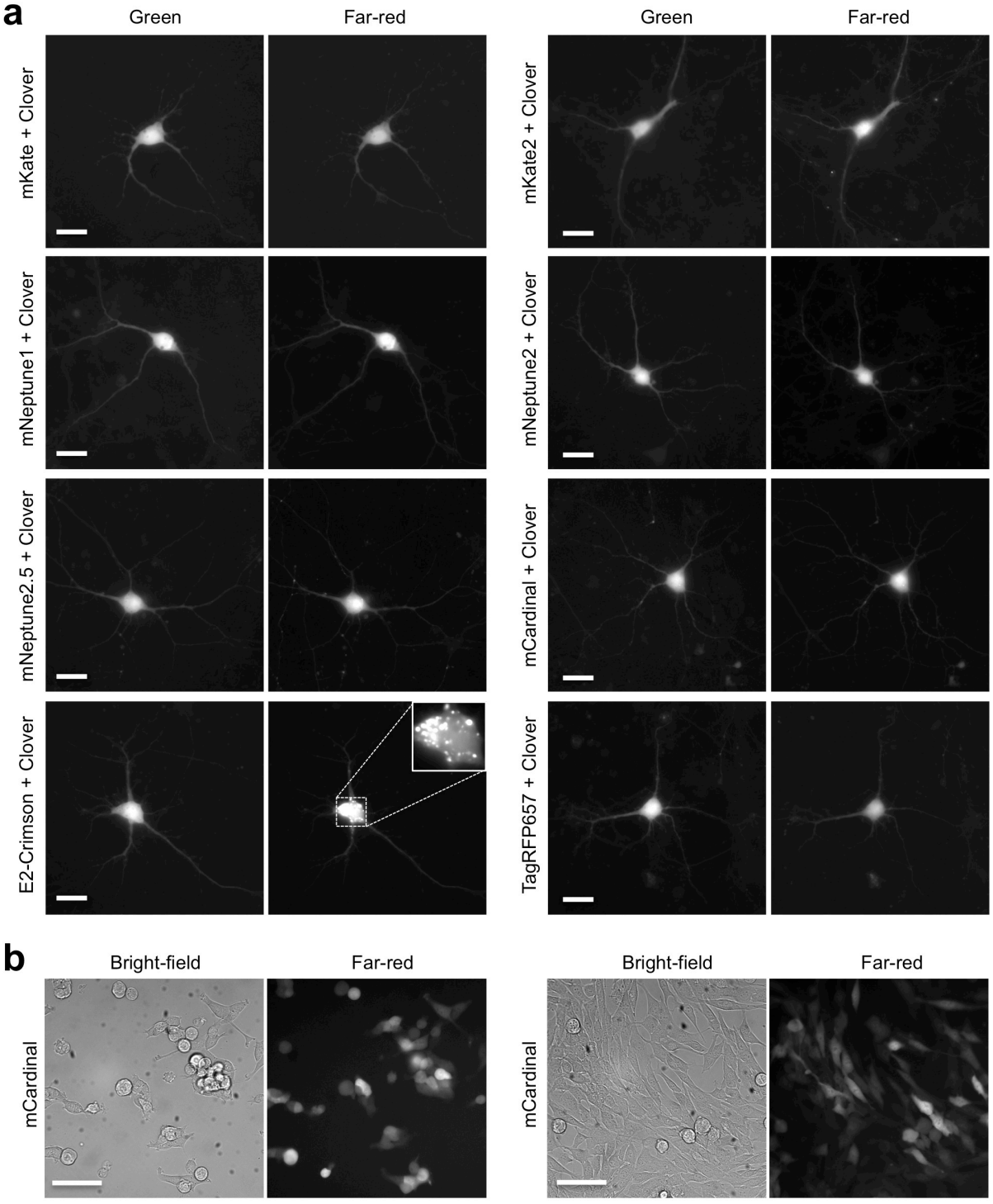

(a) Rat embryonic day 18 hippocampal neurons were cotransfected with pcDNA3-Clover and a pcDNA3 plasmid expressing a far-red FP. Imaging was performed 12 days post-transfection using a 615/30 nm excitation filter and a 675/50 nm emission filter. Scale bars, 20 μm. **(b)** mCardinal expression in undifferentiated (left) and differentiating (right) primary mouse myoblasts. Scale bars, 20 μm.

Supplementary Figure 8. Performance of mNeptune2 fusions in mammalian cells

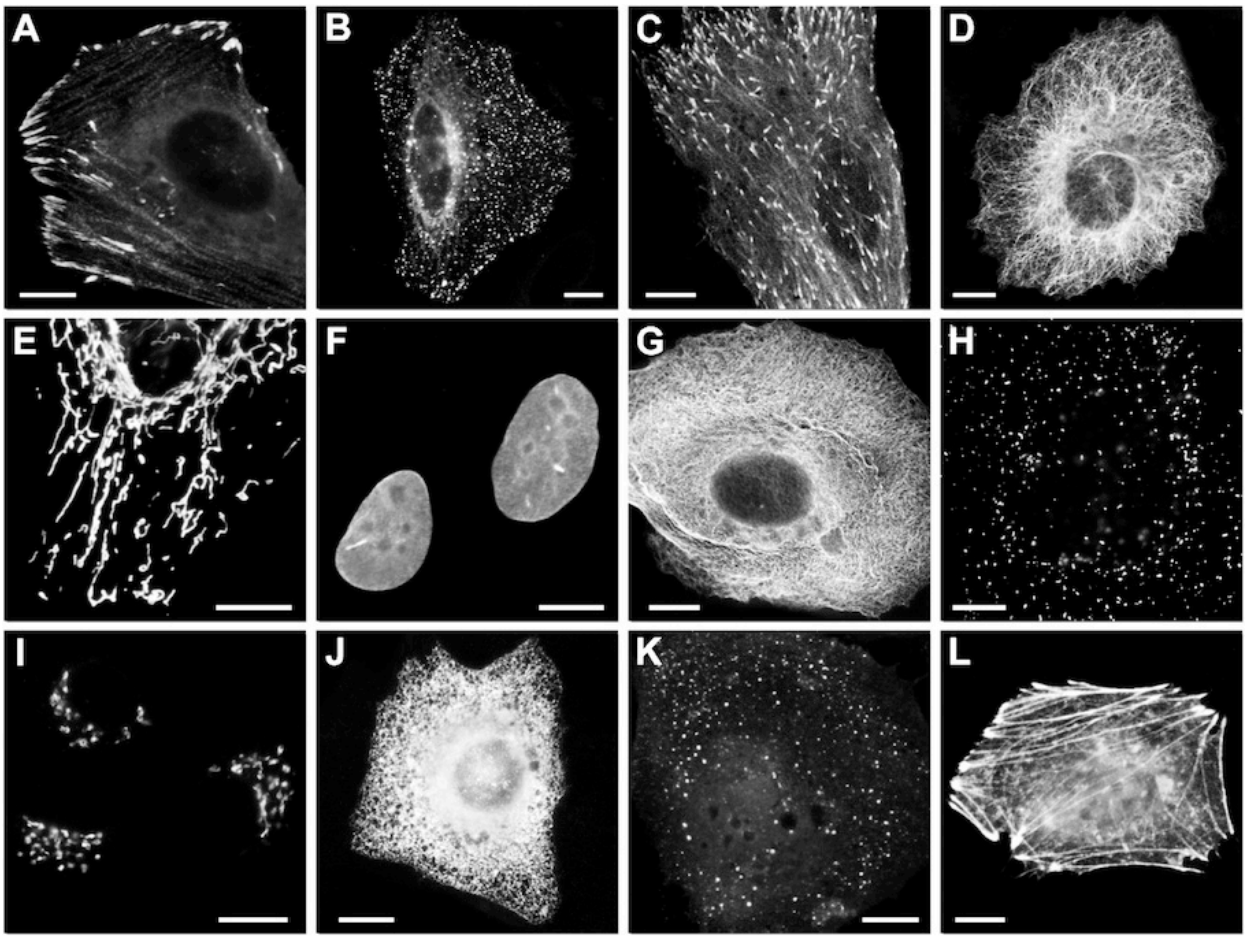

Cells were imaged with 633 nm laser excitation and a Cy5 emission filter. Fusions at the mCardinal N-terminus: **(a)** VASP-10aa-mNetpune2 (mouse; Vasodilator-stimulated phosphoprotein; focal adhesions), **(c)** EB3-7aa-mNeptune2 (human; Microtubule-associated protein RP/EB family member 3; the plus end of microtubules), **(e)** PDHA1-10aa-mNeptune2 (human; pyruvate dehydrogenase, mitochondria), **(g)** keratin-17aa-mNeptune2 (human; intermediate filaments; cytokeratin 18), **(h)** PMP-10aa-mNeptune2 (human; peroxisomal membrane protein; peroxisomes), **(i)** mannosidaseII-10aa-mNeptune2 (mouse; the Golgi complex), **(j)** calnexin-14aa-mNeptune2 (human; endoplasmic reticulum). Fusions at the mCardinal C-terminus: **(b)** mNeptune2-7aa-Rab5a (canine; Rab5a; endosomes), **(d)** mNeptune2-18aa-α-tubulin (human; microtubules), **(f)** mNeptune2-10aa-lamin B1 (human; nuclear envelope), **(k)** mNeptune2-15aa-Clathrin (human; clathrin light chain B) and **(l)** mNeptune2-18aa-β-actin (human; actin cytoskeleton). The number followed by "aa" refers to the linker length in aa. Scale bars, 10 μm.

Supplementary Figure 9. Performance of mCardinal fusions in mammalian cells

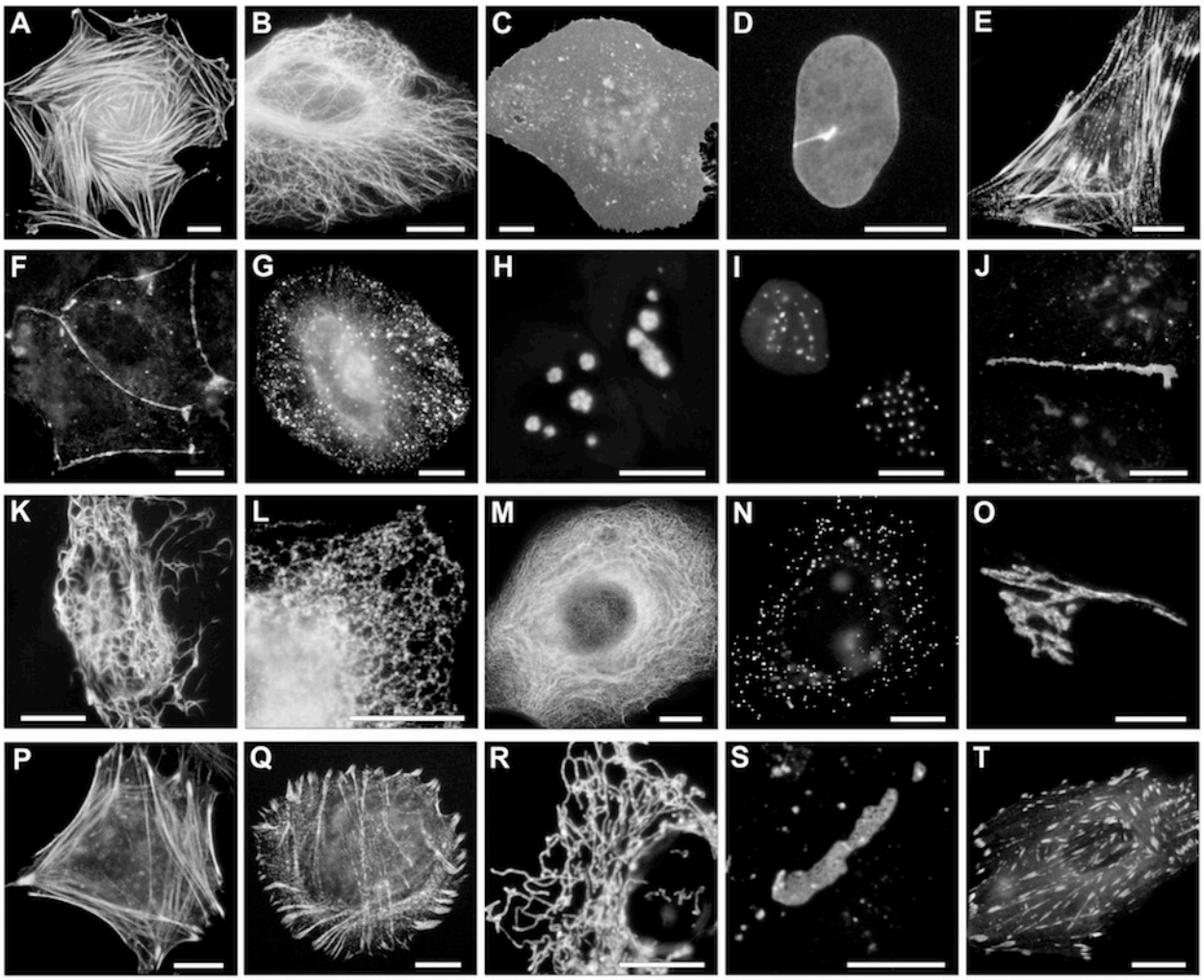

Cells were imaged with 633 nm laser excitation and a Cy5 emission filter. **(a-h)** Fusions at the mCardinal C-terminus: **(a)** mCardinal-18aa-β-actin (actin cytoskeleton), **(b)** mCardinal-18aa-α-tubulin (microtubules), **(c)** mCardinal-5aa-CAAX (20-aa H-Ras farnesylation signal, plasma membrane), **(d)** mCardinal-10aa-lamin B1 (nuclear envelope), **(e)** mCardinal-14aa-myotilin (actin cytoskeleton), **(f)** mCardinal-14aa-ZO1 (tight junctions), **(g)** mCardinal-7aa-Rab5a (endosomes), **(h)** mCardinal-7aa-fibrillarin (nucleoli). (**i-t**) Fusions at the mCardinal N-terminus: **(i)** CENPB-22aa-mCardinal (centromeres), **(j)** VE-Cadherin-10aa-mCardinal (tight junctions), **(k)** vimentin-7aa-mCardinal (intermediate filaments), **(l)** calnexin-14aa-mCardinal (endoplasmic reticulum), **(m)** cytokeratin18-17aa-mCardinal (intermediate filaments), **(n)** PMP-10aa-mCardinal (peroxisomal membrane protein), **(o)** mannosidaseII-10aa-mCardinal (Golgi complex), **(p)** Lifeact-7aa-mCardinal (yeast; actin), **(q)** α-actinin-19aa-mCardinal (actin and focal adhesions), **(r)** PDHA1-10aa-mCardinal (pyruvate dehydrogenase, mitochondria), **(s)** connexin43-7aa-mCardinal (gap junctions), **(t)** paxillin-22aa-mCardinal (focal adhesions). HeLa cells are shown except for **(f)**, in which MDCK cells are shown. All fused domains are of human species, except for **(g)** canine Rab5a, **(o)** mouse mannosidaseII, **(p)** yeast Lifeact**, (s)** rat connexin43, and **(t)** chicken paxillin. The number followed by "aa" refers to the linker length in aa. Scale bars, 10 μm.

Supplementary Figure 10. Performance of a histone-mCardinal fusion

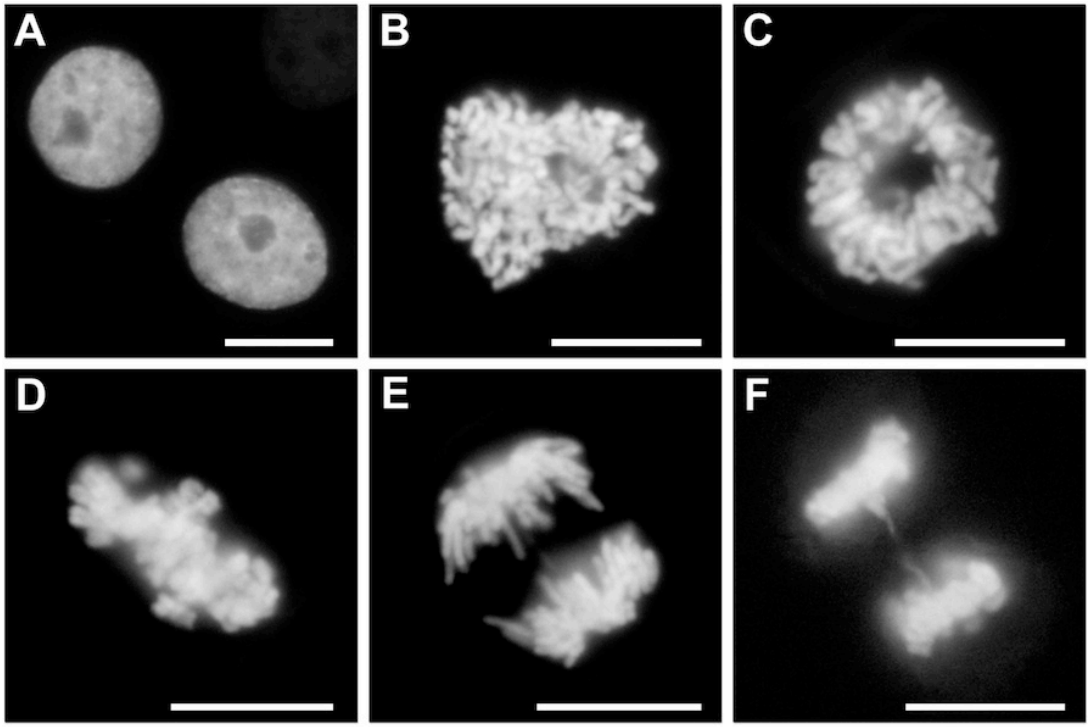

Widefield fluorescence imaging was performed on HeLa cells expressing a histone-mCardinal fusion protein with 633 nm laser excitation and a Cy5 emission filter. Human histone H1 was fused to the N-terminus of mCardinal via a 10-aa linker. (**a**) interphase, (**b**) prophase, (**c**) prometaphase, (**d**) metaphase, (**e**) anaphase, **(f)** telophase. Scale bars, 10 μm.

Supplementary Figure 11. Three-color imaging in *C. elegans* using mCardinal

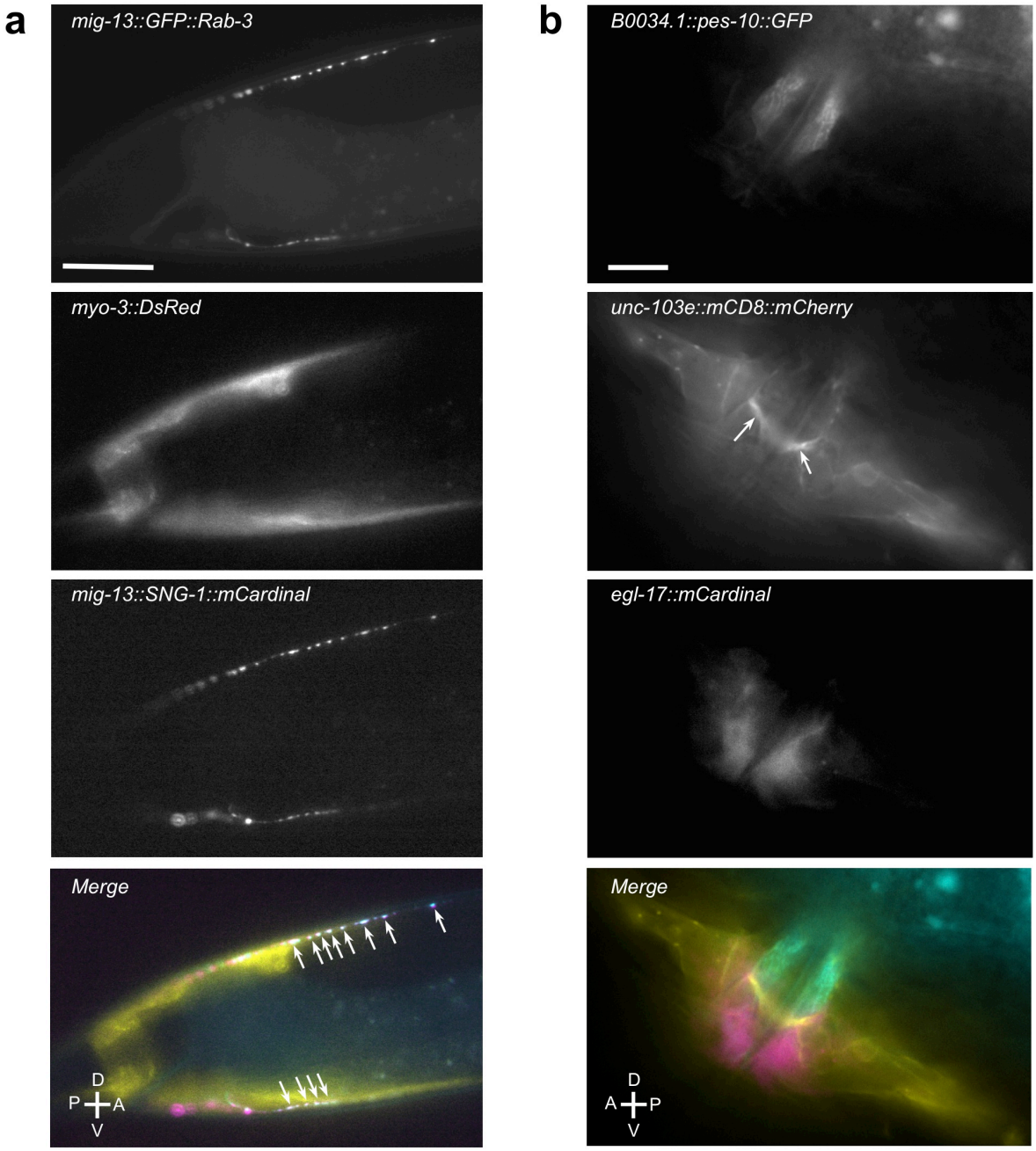

(a) Colocalization of Rab-3 (GFP::Rab-3) and synaptogyrin (SNG-1::mCardinal) in presynaptic vesicles of DA9 (dorsal) and VA12 (ventral) neurons. The fluorescent puncta correspond to presynaptic vesicles along the body wall muscles labeled with DsRed. In the merged image, pseudocolors were assigned as follows: cyan, GFP; yellow, DsRed; and Magenta, mCardinal. Arrows indicate the colocalization of Rab-3 and SNG-1. Anterior (A), posterior (P), dorsal (D), ventral (V). Scale bar, 10 μm. **(b)** Three-color imaging of vulva. Vulva muscle, primary and secondary vulva epithelial cells were labeled by mCD8::mCherry, GFP and mCardinal, respectively. Arrows indicate the muscle arms of type-2 vulval muscle (VM2). Scale bar, 5 μm.

Supplementary Figure 12. Comparison of mCardinal with iRFP in cells in deep tissue

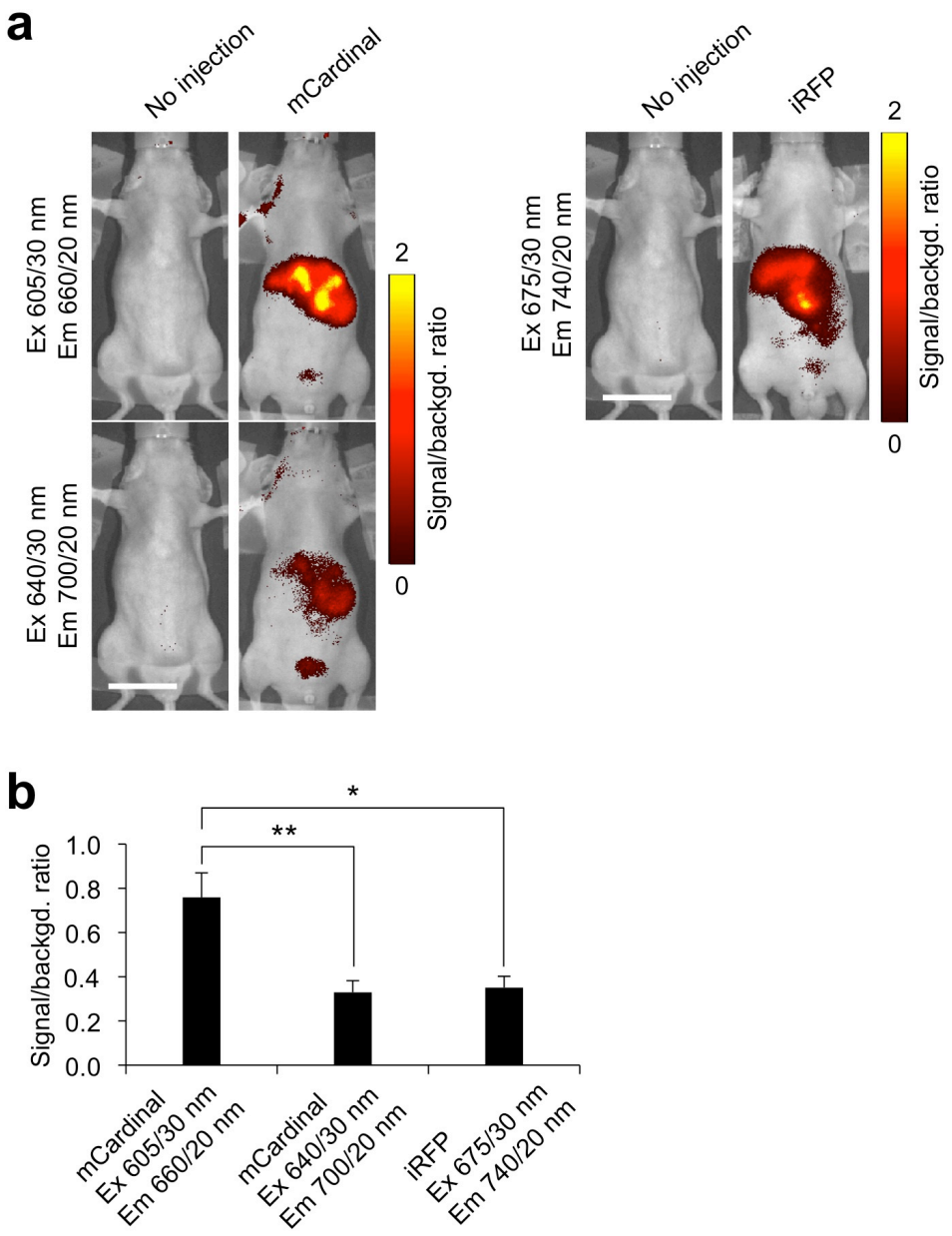

(a) Representative fluorescence images of mice expressing mCardinal or iRFP in livers. Nude mice were injected hydrodynamically with 40 µg plasmid DNA expressing FPs driven by a CAG promoter. Images were acquired in epifluorescence mode with 3 filter sets indicated in **(a)** 40 h after injection. The color bar indicates the signal/background ratio. Scale bars represent 2 cm. **(b)** Quantification of fluorescence signal over background. Bars are mean ± SEM of 4 replicates. Differences are statistically significant by one-way ANOVA ($P < 0.01$). Asterisks indicate significant differences by Tukey's multiple comparison test ($*P < 0.05$, $**P < 0.01$).

Supplementary Figure 13. Repeatability of deep-tissue fluorescence imaging

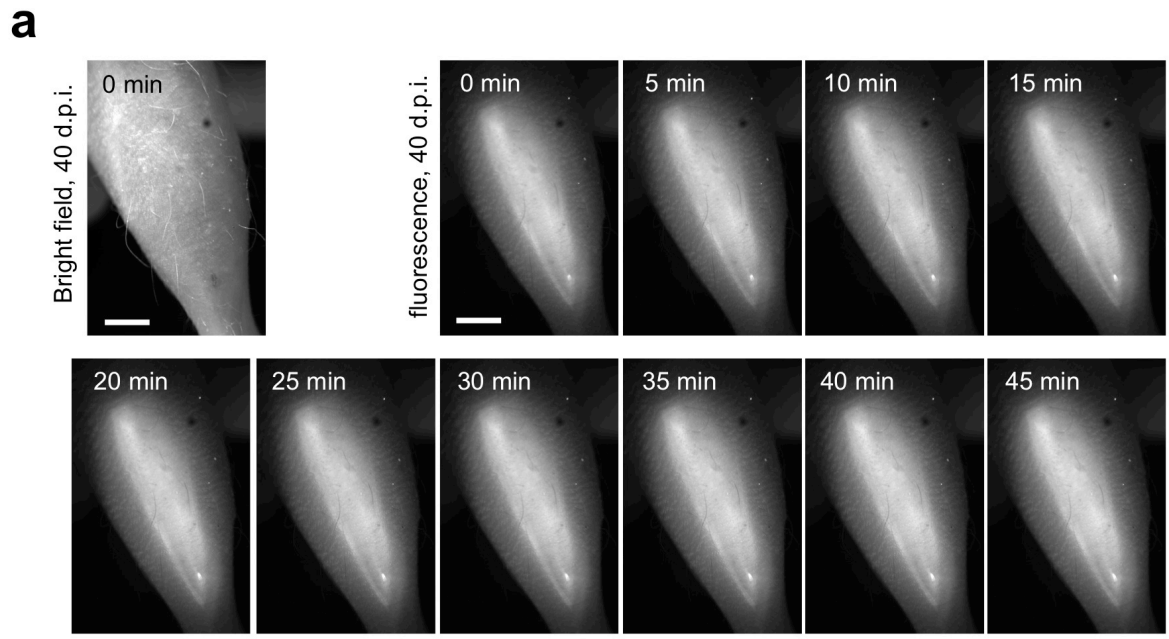

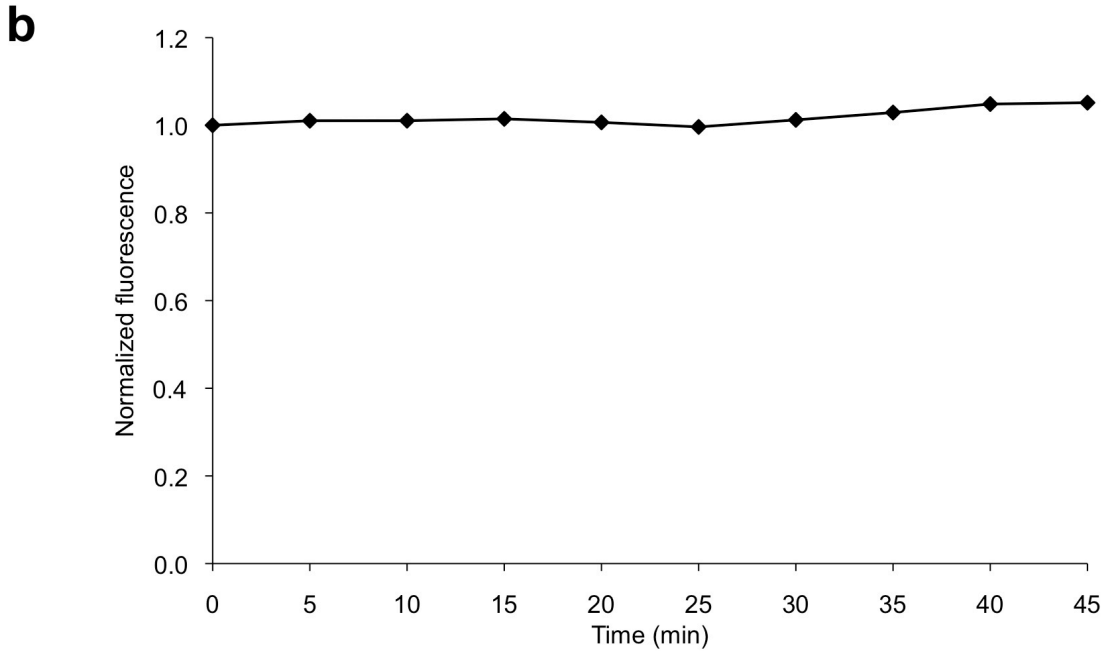

(a) Fluorescence images of mCardinal-expressing muscle fibers from the same leg with a 5 min time interval. A SCID mouse was injected with one million stable myoblasts expressing mCardinal. At 40 days after injection, the mouse was anesthetized and fluorescence images were acquired using the same imaging conditions as Fig. 4a except exposure time was increased to 20 s. Measured irradiance at the specimen plane was 3.6 mW/cm^2, corresponding to an energy exposure of 0.072 J/cm^2 per frame. Scale bars, 2 mm. **(b)** Quantification of fluorescence signal subtracted by background.

Supplementary Figure 14. Validation of minicircle constructs expressing far-red FPs and iRFP

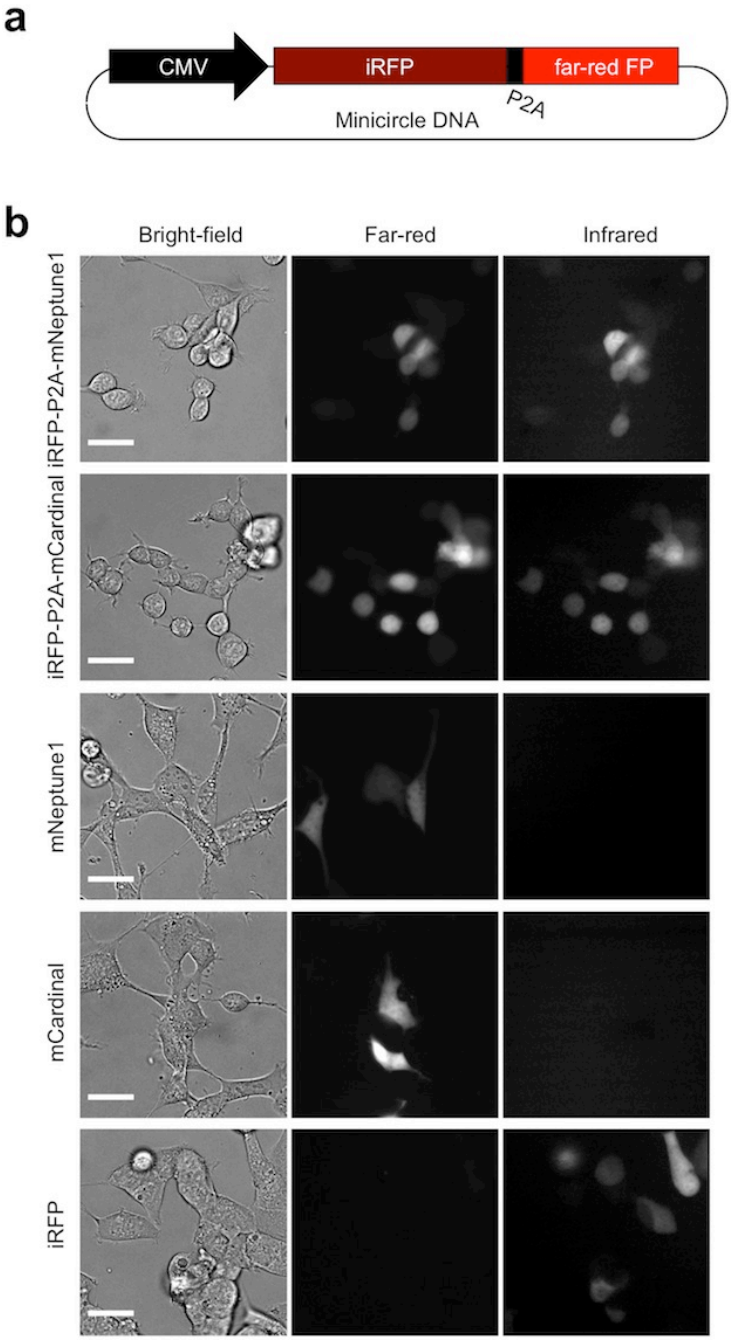

(a) Schematics of minicircles containing mNeptune1 or mCardinal and iRFP, separated with a P2A sequence. **(b)** Fluorescence images of stable myoblasts expressing the constructs shown in **(a)** (top two rows) and transiently transfected HEK293A cells with a pcDNA3 plasmid expressing FP (bottom three rows). Far-red and infrared fluorescence were acquired through far-red (615/30 nm excitation, 630 nm dichroic, and 675/50 nm emission) and infrared filters (682/22 nm excitation, 700 nm dichroic, and 710 nm longpass emission) respectively. All images are normalized to the same intensity scale. Scale bars, 20 μm.

Supplementary Figure 15. Filter sets used to image mCardinal and iRFP

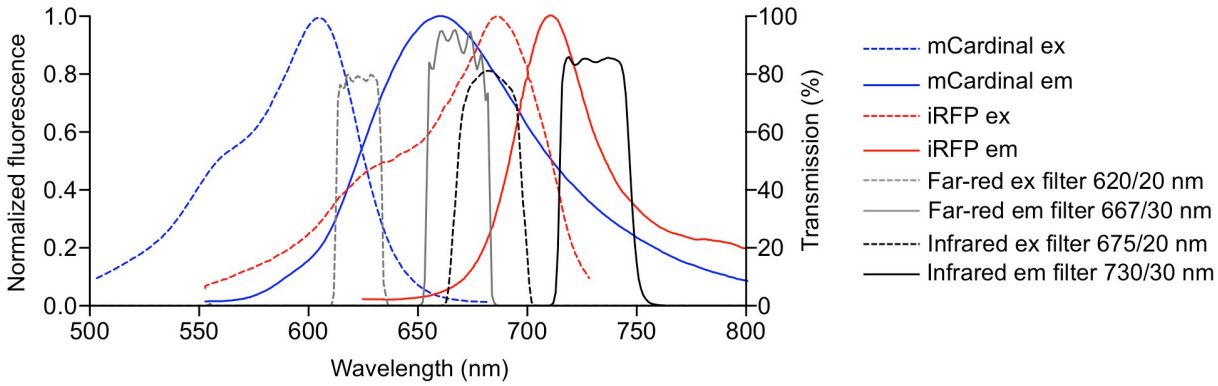

Excitation and emission spectra (left y-axis) of mCardinal and iRFP superimposed over optimized filters (right y-axis) to image far-red and infrared FPs.

Supplementary Figure 16. Constructs for expressing far-red FPs and Clover in stem cells

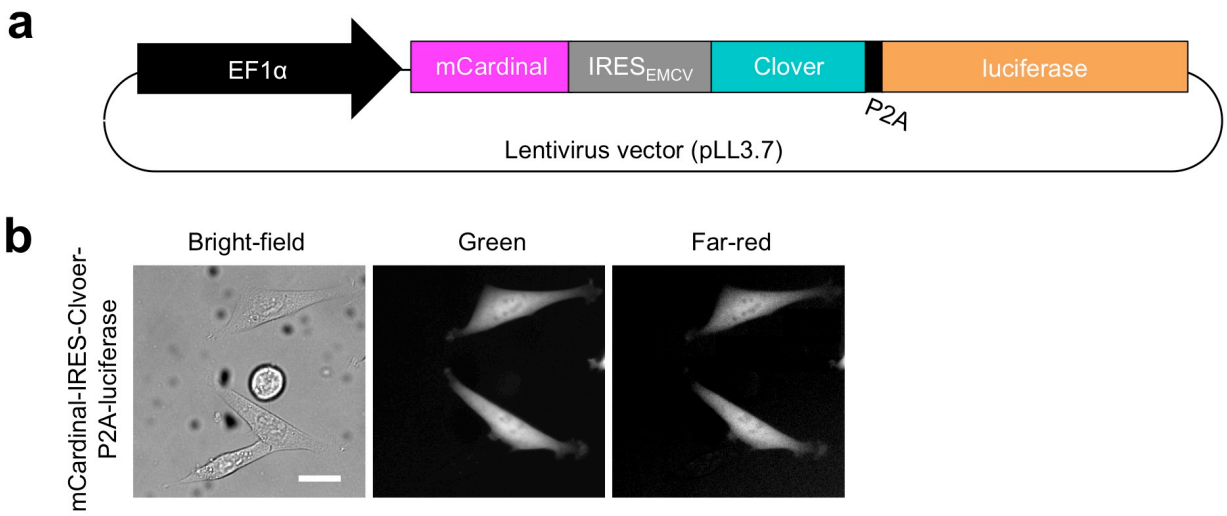

(a) Schematics of the lentivirus construct used to infect stem cells. mCardinal, Clover, luciferase are separated by an IRES element from encephalomyocarditis virus and a 2A peptide from porcine teschovirus-1, respectively. **(b)** Fluorescence images of HEK293A cells expressing the construct shown in **(a)**. Scale bar, 20 μm.

Supplementary Table 1: Data collection and refinement statistics

	mCardinal	mCardinal V218E
Data collection		
Space group	$P12_11$	$P2_12_12_1$
Cell dimensions *a*, *b*, *c* (Å)	53.2, 136.7, 167.6	72.5, 102.9, 116.5
Cell angles α, β, γ	90.0, 90.1, 90.0	90.0, 90.0, 90.0
Wavelength (Å)	1.0	1.115834
Resolution (Å)	47.56-2.21 (2.29-2.21)*	45.44-1.70 (1.80-1.70)*
R_{sym} or R_{merge}	0.132 (0.800)*	0.052 (0.574)*
$CC_{1/2}$	0.978 (0.261)*	0.999 (0.845)*
*CC**	0.994 (0.643)*	1.000 (0.957)*
$I/\sigma I$	5.61 (1.14)*	16.33 (2.21)*
Completeness (%)	94.8 (93.8)*	98.6 (96.3)*
Redundancy	1.9 (1.9)*	4.12 (4.14)*
Refinement		
$R_{work/}$ R_{free}	0.2225/0.2511	0.1600/0.1934
R.m.s deviations, bond lengths (Å)	0.004	0.012
R.m.s deviations, bond angles (°)	0.85	1.34

*Highest resolution shell is shown in parenthesis.

Supplementary Video 1. Time-lapse laser-scanning confocal fluorescence microscopy imaging of a mCardinal-18aa-actin fusion protein targeting actin filaments in a fox lung fibroblast. Frames were acquired 18 s apart with a 633 nm laser and a 60× objective. Playback was encoded at 15 frames per s.

Supplementary Video 2. Time-lapse laser-scanning confocal fluorescence microscopy imaging of a PDHA1-10-aa-mCardinal fusion protein targeting mitochondria in an NIH3T3 fibroblast. Frames were acquired 15 s apart with a 633 nm laser and a 60× objective. Playback was encoded at 15 frames per s.

Supplementary Video 3. Fast time-lapse laser-scanning confocal fluorescence microscopy imaging of freely moving *C.elegans* with mCardinal-labeled pharynx. Frames were acquired 125 ms apart with a 635 nm laser and a 20× objective (NA=0.75). Power measured at the specimen was 100 μW, corresponding to an irradiance of 0.030 J/cm^2 per frame. Playback was encoded at 7 frames per s.

Supplementary Video 4. Fast time-lapse laser-scanning confocal fluorescence microscopy imaging of partially immobilized *C.elegans* with mCardinal-labeled pharynx. Worms were partially immobilized by dotting cyanoacrylate glue on their tails. 1 mg/mL serotonin in M9 was added to keep the sample hydrated during recordings and to induce pharyngeal pumping. Frames were acquired 125 ms apart with a 635 nm laser and a 20× objective (NA=0.75). Power measured at the specimen was 100 μW, corresponding to an irradiance of 0.030 J/cm^2 per frame. Playback was encoded at 7 frames per s.